Enhancement of the Erbium Concentration in $RbTiOPO_4$ by Codoping with Niobium

J. J. Carvajal,[†] V. Nikolov,[‡] R. Solé,[†] Jna. Gavaldà,[†] J. Massons,[†] M. Rico,[§] C. Zaldo,[§] M. Aguiló,[†] and F. Díaz*,[†]

Laboratori de Física Aplicada i Cristal·lografia, Universitat Rovira i Virgili, 43005 Tarragona, Spain, Institute of General and Inorganic Chemistry, Bulgarian Academy of Sciences, 1040 Sofia, Bulgaria, and Instituto de Ciencia de Materiales de Madrid, Consejo Superior de Investigaciones Científicas, Cantoblanco, 28049 Madrid, Spain

Received April 13, 2000. Revised Manuscript Received July 31, 2000

A thorough study of the $RbTiOPO_4$ (RTP) crystallization in its self-flux and WO_3-containing fluxes (10, 20, and 30 mol % WO_3) has been performed. The composition regions and isotherms of crystallization were obtained, and most of the crystallized neighboring phases were identified. Afterward, the possibilities of doping and codoping RTP crystals with Er^{3+} and Nb^{5+} were studied. Adding Nb_2O_5 substituting TiO_2 in the solution increases the distribution coefficient of Er^{3+} but changes the crystal morphology toward thin plates significantly. This means it is difficult to grow crystals of sufficient quality and size for research and applications. To optimize the crystal growth process, the conditions for growing doped and codoped RTP single crystals with Er^{3+} and Nb^{3+} by the top seeded solution growth technique (TSSG) were studied. For crystal growth from self-flux, stirring the solution with an immersed platinum turbine significantly increased the efficiency of the crystal growth process. These conditions allow achieving 0.65×10^{20} atom·cm^{-3} as an Er^{3+} dopant concentration in the crystal. The Judd−Ofelt parameters for Er^{3+} in RTP:Nb determined from the 300 K optical absorption spectra are $\Omega_2 = 5.99 \times 10^{-20}$, $\Omega_4 = 0.54 \times 10^{-20}$, and $\Omega_6 = 0.37 \times 10^{-20}$ cm^2. Finally, the second harmonic generation (SHG) efficiency of RTP:Nb single crystals increased as the concentration of Nb increased up to a 4 atom % of Ti^{4+} substitution, after which the SHG efficiency decreased.

Introduction

Rubidium titanyl phosphate, $RbTiOPO_4$ (RTP), like $KTiOPO_4$ (KTP) and many of their isostructural materials, has important applications in nonlinear optics and electrooptics due to its high nonlinear optical and electrooptical coefficients, high optical damage threshold, low dielectric constant, and chemical stability.[1,2]

Doping KTP single crystals with different elements has recently been investigated to improve several properties such as the ionic conductivity along the *c* direction,[3−5] the reduction of the KTP cutoff wavelength to allow noncritical type II phase matching below 990 nm of the fundamental radiation,[6,7] and so forth. Doping with rare earth (RE^{3+}) ions is particularly interesting because of the possibility of merging the ion photoluminescence and the NLO properties of the matrix to achieve self-induced effects. In particular, the laser 1.5 and 2.9 μm emissions of Er^{3+} are interesting for optical communications and medical applications.[8]

RE^{3+} doping of KTP has already been investigated by us in previous works.[9,10] The RE^{3+} distribution coefficients were very low, typically about 10^{-3}. However, the presence of codopants generally increased the distribution coefficient of the RE^{3+}. Codoping with Nb^{5+} is one of the most effective methods, but the RE concentrations so far achieved in KTP are not high enough to obtain efficient fluorescence from the RE's. Our previous work showed that codoping with Rb^+ also increases the incorporation of RE^{3+} into the crystal, which suggests that the distribution coefficient of RE^{3+} in RTP could be significantly higher than that in KTP.

The aim of this paper is to study the possibilities for doping RTP with Er^{3+}, which has a middle ionic radius in the rare earth family[11] and is one of the most widely used ions in laser technology. The RTP codoping with Er^{3+} and Nb^{5+} is also studied in order to increase the

* Corresponding author. E-mail: diaz@quimica.urv.es.
[†] Universitat Rovira i Virgili.
[‡] Bulgarian Academy of Sciences.
[§] Instituto de Ciencia de Materiales de Madrid, Consejo Superior de Investigaciones Científicas.

(1) Hagerman, M. E.; Poeppelmeier, K. R. *Chem. Mater.* **1995**, *7*, 602.
(2) Satyanarayan, M. N.; Deepthy, A.; Bhat, H. L. *Crit. Rev. Solid State Mater. Sci.* **1999**, *24*, 103.
(3) MacGee, T. F.; Blom, G. M.; Kostecky, G. J. *J. Cryst. Growth* **1991**, *109*, 361.
(4) Bolt, R. J. *J. Cryst. Growth* **1993**, *126*, 175.
(5) Hörlin, T.; Bolt, R. *Solid State Ionics* **1995**, *78*, 55.
(6) Cheng, L. T.; Cheng, L. K.; Harlow, R. L.; Bierlein, J. D. *Appl. Phys. Lett.* **1994**, *64*, 155.
(7) Anderson, M. T.; Phillips, M. L. F.; Stucky, G. D. *J. Non-Cryst. Solids* **1994**, *178*, 120.
(8) Koechner, W. *Solid-State Laser Engineering*; Springer Series in Optical Sciences; Springer-Verlag: Berlin, 1996; pp 63−66.
(9) Solé, R.; Nikolov, V.; Koseva, I.; Peshev, P.; Ruiz, X.; Zaldo, C.; Martín, M. J.; Aguiló, M.; Díaz, F. *Chem. Mater.* **1997**, *9*, 2745.
(10) Zaldo, C.; Rico, M.; Diaz, F.; Carvajal, J. J. *Opt. Mater.* **1999**, *13*, 175.
(11) Shannon, R. D. *Acta Crystallogr.* **1976**, *A32*, 751.

10.1021/cm000305c CCC: $19.00
Published on Web 09/23/2000

Table 1. Data Associated with Doping and Codoping in RTP[a]

experiment	dopants	Rb_2O/P_2O_5	$(Rb_2O + P_2O_5)/(TiO_2 + X)$ X = Er_2O_3, Nb_2O_5, or $Er_2O_3 + Nb_2O_5$	crit conc	K_{Er}	K_{Nb}
I	Er	55/45	78/22	2	0.02	
II	Er	57.5/42.5	75/25	8	0.02	
III	Er	60/40	75/25	>5		
IV	Nb	55/45	78/22	>14	0.5	
V	Er + Nb	55/45	78/22	14	0.12	0.43
VI	Er + Nb	57.5/42.5	75/25	9	0.17	0.45
VII	Er + Nb	60/40	75/25	6	0.35	0.5

[a] Note: The critical concentration in the flux is defined as 100(maximum doping oxide)/(maximum doping oxide + TiO_2)(mol %). For experiments V, VI, and VII the concentration corresponds to Nb.

erbium concentration in the crystal. Because of the scarce information in the literature about RTP crystal growth, the crystallization region of RTP in the self-flux and in WO_3-containing solutions was also determined in this work. Finally, several optical properties such as absorption spectra and second harmonic generation (SHG) of the doped RTP crystals are also studied.

Experimental Procedures

RTP Crystallization Regions. To determine the concentration region and crystallization temperatures of the $RbTiOPO_4$ phase in the self-flux and in WO_3-containing fluxes, different solution compositions were investigated. The experiments were carried out in a vertical tubular furnace controlled by an Eurotherm 818P controller/programmer, using 25 cm^3 platinum crucibles filled with 15−20 g of solution. Rb_2CO_3, $NH_4H_2PO_4$, TiO_2, and WO_3 (p.a.) were mixed in the desired ratios and used as initial reagents.

The mixed reagents were decomposed by heating them until bubbling of NH_3, H_2O, and CO_2 was complete. The solution was homogenized by maintaining the temperature at about 50−100 °C above the expected saturation temperature for 3−5 h. The axial temperature difference in the solution was about 15 °C, and the center of the solution surface was colder than any other part of the volume. The temperature of the homogeneous solution was lowered in ∼10 °C steps every 30 min, until crystals appeared on a platinum wire immersed in the solution. The crystallized phase was identified by X-ray diffraction analysis and electron probe microanalysis (EPMA), and the shape of the crystals was observed by optical and electron microscopies. At the same time, information about the saturation temperature of the solution, T_s, was obtained. More accurate measurements of T_s were then taken by observing the growth or dissolution of an RTP seed on contact with the solution surface.

After studying about 30−40 different compositions of the solution for each flux used, the crystallization region and the saturation temperature of RTP in the self-flux and in solutions containing 10, 20, and 30 mol % WO_3 were obtained.

RTP Doping and Codoping with Er^{3+} and Nb^{5+}. The solution compositions shown in Table 1 (columns C and D) were chosen as reference compositions to investigate the critical concentration of the Er_2O_3, Nb_2O_5, and $Er_2O_3 + Nb_2O_5$, which allow the crystallization of RTP as the first and only crystallized phase in the self-flux. When double substitution ($Nb_2O_5 + Er_2O_3$) was used, the concentration of Er_2O_3 was fixed at 2 mol % substituting TiO_2, and the critical concentration of Nb_2O_5 was obtained. The reagents used to dope and codope the RTP were Nb_2O_5 and Er_2O_3 (99.9%). All this research was performed under the same conditions as the determination of the RTP crystallization regions (homogenization of the solution, temperature distribution in the crucible, cooling, etc.), and the concentration of doping elements was increased until a new crystal phase appeared.

X-ray Powder Diffraction. The X-ray powder diffraction technique was used to identify the RTP and neighboring phases of the crystallization regions determined and to determine the evolution of the cell parameters with the concentration of Nb^{5+} in the RTP crystals. We used a Siemens D5000 powder diffractometer in a $\theta-\theta$ configuration using the Bragg−Brentano geometry. The crystal cell parameters of the RTP doped with Nb^{5+} were calculated from the diffraction data, obtained at $2\theta = 10-70°$, ss = 0.02°, st = 16 s, using the FULLPROF program[12] and the Rietveld method.[13] The coordinates of the atoms in the RTP lattice taken from a previous paper[14] were used as the starting model for the calculations. A Pearson VII function was selected to describe individual line profiles, and the final Rietveld refinement included the following parameters: the zero-point, the scale factor, one or three background coefficients, the three cell parameters, three half-width parameters and one profile shape parameter. About 400 reflections were used in all cases.

Dopant Concentration Analyses. RTP single crystals, obtained with different concentrations of dopants, were separated and cleaned. Some were analyzed by EPMA to obtain the concentration of the doping elements in the RTP crystals. A Cameca CAMEBAX SX-50 was used. Some of these crystals were also analyzed by inductively coupled plasma (ICP) and atomic absorption spectroscopy (AAS) using Jobin Ybon France JY-38 ICPA and PYE UNICAM SP-192 AAS equipment, respectively.

Top Seeded Solution Growth (TSSG). To obtain inclusion-free single crystals of a size suitable for optical investigation, different growth experiments were performed by the top seeded solution growth (TSSG)/slow cooling technique. A vertical tubular furnace, controlled by a Eurotherm 818P controller/programmer was used. The solutions were prepared in conical platinum crucibles of 25 cm^3 by mixing the appropriate amounts of reagents to obtain the compositions shown in Table 2. The axial temperature difference in the solutions was about 10 °C. The bottom of the solution was warmer than the surface. The crystals were grown with *c*-oriented RTP seeds fixed in a growth device made up of a platinum turbine with two seeds symmetrically located with respect to the rotation axis and displaced some millimeters from this axis. Crystals in WO_3 flux, however, were grown on *c*-oriented RTP seeds located at the center of the solution surface without additional stirring of the solution. This growth device is shown in Figure 1. The *a* direction of the seeds was always placed on the radial direction of the rotation movement. The saturation temperature was determined by observing the dissolution or growth of both seeds in contact with the surface of the solution. During the growth processes the temperature was reduced 12 °C at a rate of 1 °C/day, except for the crystals grown in WO_3 flux, in which the temperature was decreased by 30 °C at a rate of 0.1 °C/h. The velocity of rotation was maintained constant at 65 rpm for all experiments.

Optical Absorption. Optical absorption studies were performed on RTP:Er,Nb crystals with a Varian Cary 500 Scan spectrophotometer. These crystals were cut as thin plates of 2 mm thickness, parallel to the {100} face, and polished to

(12) Rodriguez-Carvajal, J. *Short reference guide of the program FULLPROF*; Laboratoire Leon Brillouin: 1998.
(13) Young, R. A. *The Rietveld Method*; Oxford Science Publication, International Union of Crystallography: 1995.
(14) Thomas, P. A.; Mayo, S. C.; Watts, B. E. *Acta Crystallogr.* **1992**, *B48*, 401.

Table 2. Growth Data Associated with Er- or Nb-Doped and Codoped RTP Single Crystals

exp no.	solution composition $Rb_2O-P_2O_5-TiO_2-Er_2O_3-Nb_2O_5-WO_3$	solution wt (g)	$\Delta T_{saturation}$ (°C)	efficiency (%)	crystal dimensions ($a \times b \times c$) (mm)	cryst wt (g)	avg supersaturation (g/°C × 100 g solution)
1	42.9−35.1−22−0−0−0	40			9.8 × 6.6 × 6.2 5 × 6 × 6	0.879	
2	43.1−31.9−24.5−0.5−0−0	41	5.5	45.8	5.8 × 8.6 × 6.2 4.9 × 7 × 5.1	0.845	0.370
3	42.9−35.1−21.6−0−0.44−0	41.5			2.5 × 6 × 5 4.3 × 7.3 × 6.5	0.475	
4	42.9−35.1−20.7−0−1.32−0	44	2	18.2	2.8 × 5 × 5 1.5 × 4 × 3	0.163	0.170
5	42.9−35.1−20.9−0.44−0.66−0	29.5	4	50	2.1 × 5.5 × 5.2 2.2 × 5 × 4.5	0.260	0.122
6	42−28−28.5−0.6−0.9−0	28	1.5	12	2.4 × 2.3 × 2.8 1.9 × 1.9 × 2.1	0.040	0.096
7	41.2−33.7−23.7−0.5−0.75−0	37	6.5	59	2.5 × 5 × 5 2.7 × 4.5 × 4.5	0.237	0.100
8	44.4−29.6−24.7−0.52−0.78−0	26	1	8.3	1.6 × 1.4 × 1.4 1.6 × 3 × 1.4	0.024	0.092
9	44.2−18.9−16.8−0−0−20	34.5	8.5	28	6.5 × 8.1 × 16.4	1.301	0.440
10	44.2−19−16−0.34−0.50−20	35	6	20	2.6 × 9.2 × 5.9	0.295	0.130

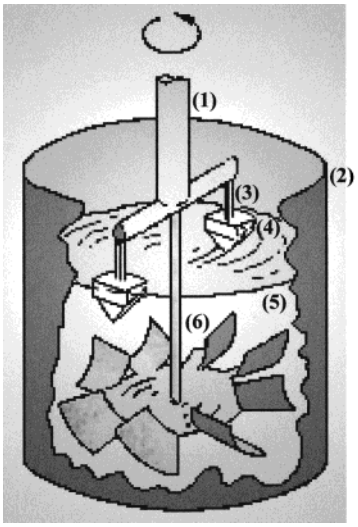

Figure 1. Accentric crystal growth system used in experiments of top seeded solution growth (TSSG).

optical quality using alumina powders. The sample studied has 2 atom % Er^{3+} that substitutes Ti^{4+} measured by EPMA. From these results and the calculated cell volume, the Er^{3+} concentration per volume unit is 0.65×10^{20} atoms·cm^{-3}. The spectra were collected at room temperature in the 350−1750 nm range using unpolarized light propagating along the crystal *a* axis.

Second-Harmonic Generation. The SHG properties of RTP:Nb were analyzed using the powder technique.[15] The samples were prepared from powdered single crystals. This was graded between 5 and 20 μm by standard sieves and loaded into a 2 mm thick quartz cell with the aid of a vibrator to ensure uniform packing. The powder was illuminated with a YAG:Nd pulsed laser. The fundamental power was estimated by measuring the 1064 nm energy reflected by the sample. The backscattered harmonic power generated by the sample was collected by a lens and focused on a Si detector. Interferometric filters were used to select the desired signal. These signals were analyzed by a digital oscilloscope, and the ratio between the two maxims was used to describe the efficiency of the SHG process. This ratio was averaged over 100 laser shots. This method does not allow the absolute efficiency of SHG of the sample to be measured, so the SHG of RTP and that of RTP:Nb are compared with that of pure KTP, which is well established in the literature.[16]

(15) Kurtz, S. K.; Perry, T. T. *J. Appl. Phys.* **1968**, *39*, 3798.

Results and Discussion

Crystallization Regions of RTP. Figure 2 shows the crystallization region of RTP in the self-flux and the saturation temperature isotherms. SEM images of RTP and neighboring phases of this crystallization region are also shown. The crystallization region of RTP in the self-flux extends from a Rb_2O/P_2O_5 molar ratio of 52/48 to 65/35, approximately, and a concentration of TiO_2 higher than 15 mol % and up to more than 35 mol %. The RTP saturation temperature ranges from under 850 °C to over 1000 °C, and the saturation temperature isotherms are approximately parallel to the border of the crystallization region of RTP in the region rich in Rb_2O.

The neighboring phases identified in this case are TiO_2 (rutile) in the region poor in P_2O_5 and rich in TiO_2, and $Rb_3Ti_3O(P_2O_7)(PO_4)_3$ in the region rich in P_2O_5 and poor in Rb_2O. In the region poor in TiO_2 and rich in Rb_2O, highly hygroscopic and water soluble phases appear. Because of their hygroscopic nature, these phases are still unidentified.

Figures 3−5 show the crystallization regions of RTP in solutions containing 10, 20, and 30 mol % WO_3, respectively, and the saturation temperature isotherms. SEM images of the identified new neighboring phases of these crystallization regions are also shown. Comparing the RTP crystallization region in the system $Rb_2O-P_2O_5-TiO_2$ with the new ones when WO_3 is present in the solutions, a displacement to Rb_2O rich regions is observed when the concentration of WO_3 increases. The RTP crystallization region with 30 mol % WO_3 in the solution is significantly narrower than those obtained with lower WO_3 contents, and for solutions containing a higher mole % of WO_3 this region is expected to disappear. As in the previous case, the saturation temperature isotherms in these crystallization regions are parallel to the RTP crystallization boundary in the Rb_2O rich region. The saturation temperature decreases slightly when the concentration of WO_3 increases, especially to above 20 mol %.

When there is enough quantity of WO_3 in the solution, a neighboring new phase appears in the region that is

(16) Dmitriev, V. G.; Gurzadyan, G. G.; Nikogosyan, D. N. *Handbook of Nonlinear Optical Materials*; Springer-Verlag: 1991.

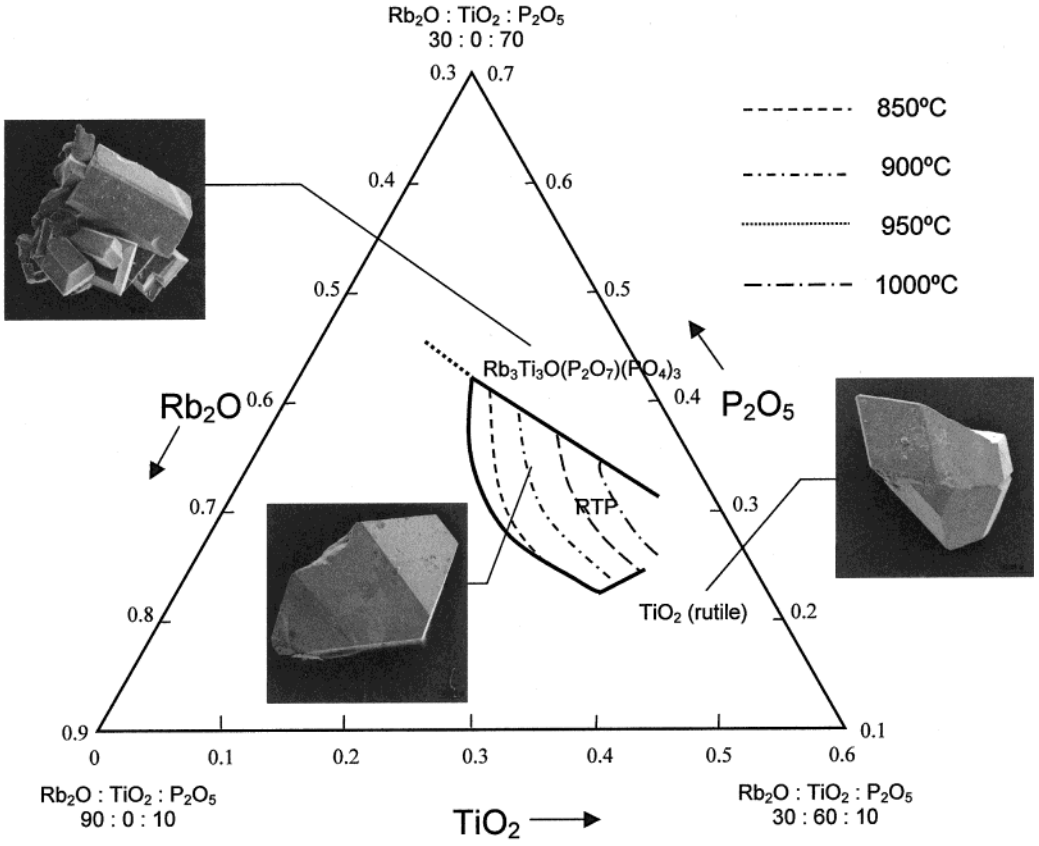

Figure 2. Crystallization region of RTP and saturation temperature in the system $Rb_2O-P_2O_5-TiO_2$. SEM images of RTP and neighboring phases.

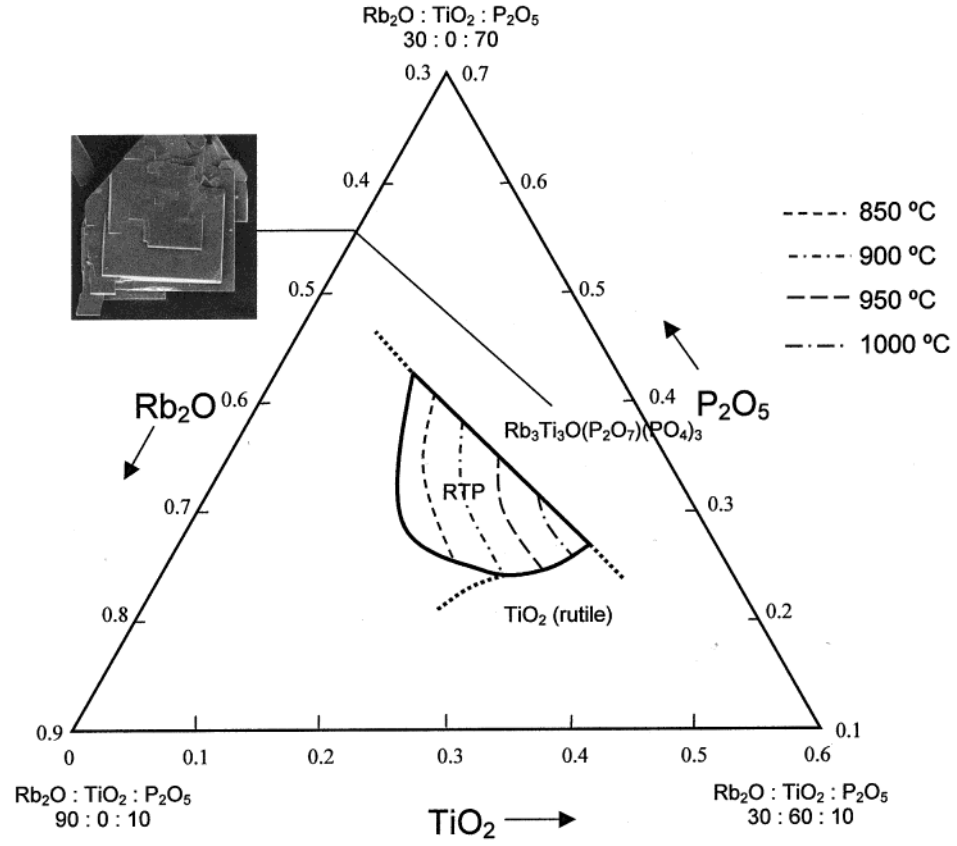

Figure 3. Crystallization region and saturation temperature of RTP in the system $Rb_2O-P_2O_5-TiO_2-WO_3$ with 10 mol % WO_3. SEM image of $Rb_3Ti_3O(P_2O_7)(PO_4)_3$.

poor in Rb_2O. This phase was identified by EPMA and X-ray powder diffraction as $RbTiPO_5$–W. For solution concentrations of WO_3 above 30 mol %, the $Rb_3Ti_3O(P_2O_7)(PO_4)_3$ phase disappeared as the neighboring

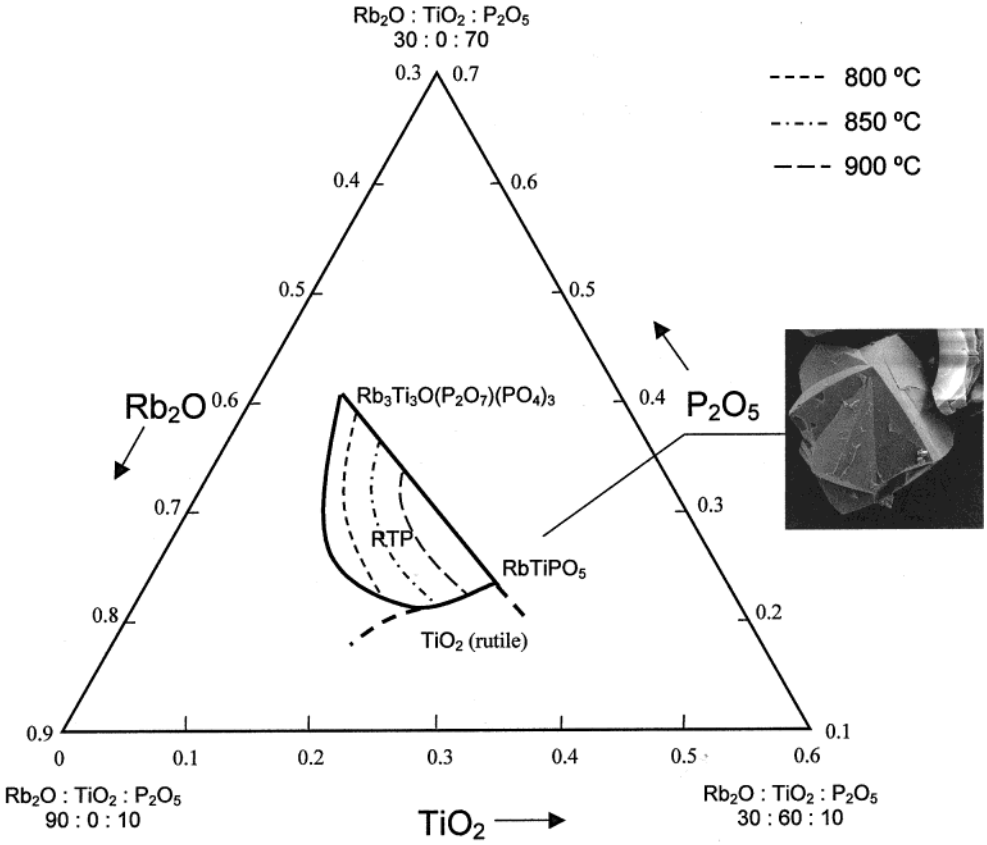

Figure 4. Crystallization region and saturation temperature of RTP in the system $Rb_2O-P_2O_5-TiO_2-WO_3$ with 20 mol % WO_3. SEM image of the $RbTiPO_5$–W phase.

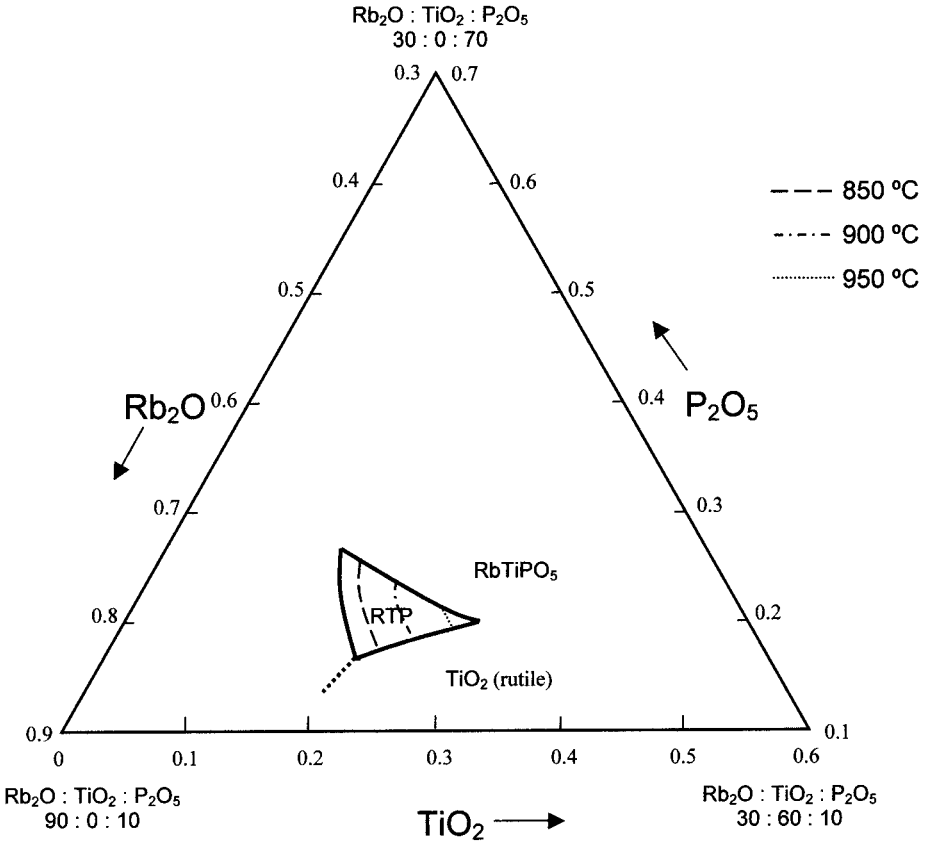

Figure 5. Crystallization region and saturation temperature of RTP in the system $Rb_2O-P_2O_5-TiO_2-WO_3$ with 30 mol % WO_3.

phase and only the $RbTiPO_5$ phase was found. It has been observed that the morphology of $Rb_3Ti_3O(P_2O_7)(PO_4)_3$ is different for solutions with and without WO_3. In WO_3-free solutions, transparent, crystalline, and

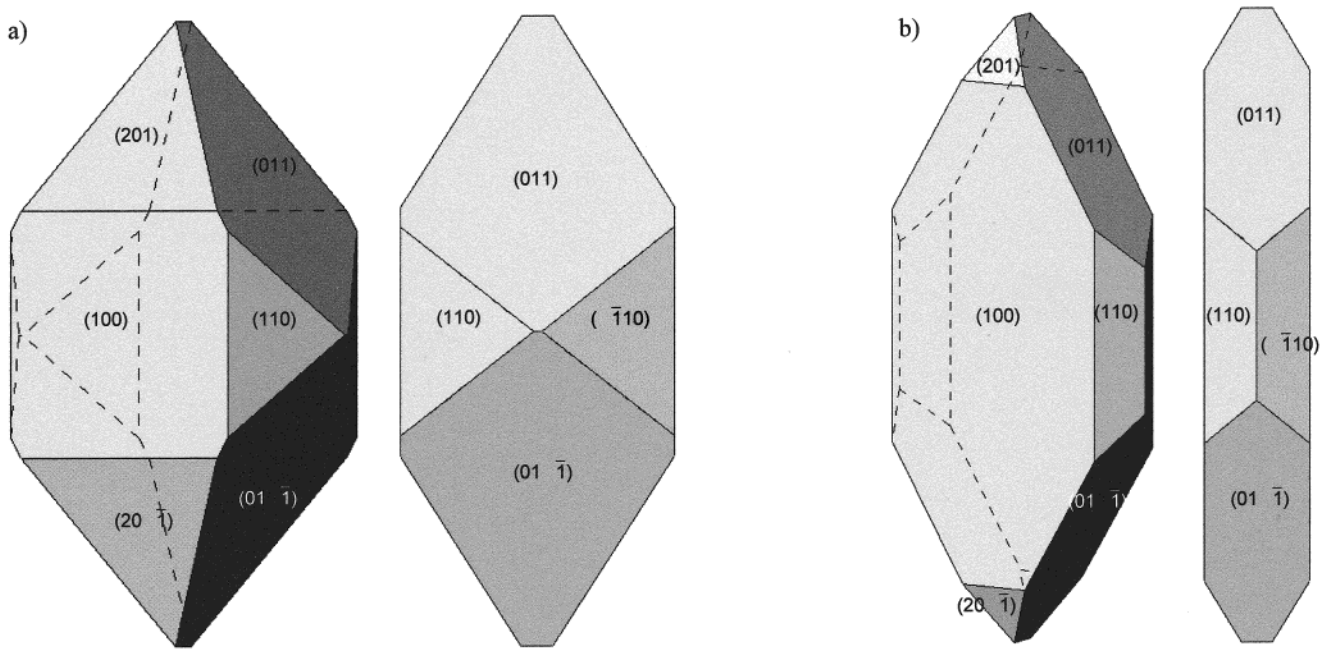

Figure 6. Morphology of (a) the RTP crystal and (b) the RTP:Nb,Er crystal.

colorless prisms appear, while, in solutions containing WO_3, this phase grows as opaque and violet crystalline thin plates. This phase was identified by EPMA and, since its X-ray powder diffraction file is not yet published, by comparing the experimental X-ray powder pattern with another calculated from the structural data of the bibliography.[17,18]

Er^{3+} Doping of RTP. The critical concentration of erbium and/or niobium below which the RTP phase can be obtained and above which other phases appear is a very important parameter for growing RTP:Er, RTP:Nb, and RTP:Er,Nb crystals. For this purpose, compositions with a saturation temperature of around 900 °C (see Table 1) were chosen. This is because at lower temperatures viscosity is expected to increase quickly and at higher temperatures the creeping of the solution increases. In these studies, solutions containing WO_3 were not used, so that the results could only be attributed to the Nb^{5+} and/or Er^{3+} ions.

The critical concentrations of Er_2O_3, Nb_2O_5, or (Nb_2O_5 + Er_2O_3) substituting TiO_2 in the solution are summarized in Table 1. For the codoping with Nb and Er, the Er_2O_3 concentration in the solution was fixed as 2 mol % Er_2O_3 substituting for TiO_2, and the critical concentration of Nb_2O_5 was obtained.

With RTP:Er crystals, the critical concentration of Er_2O_3 in the solution is enhanced when the composition of the solution contains less P_2O_5 and more TiO_2. Moreover, when the Er_2O_3 concentration in the solution increases, the time and the temperature of homogenization of the solution also increase. For concentrations of Er_2O_3 higher than the critical one, a new phase identified as $Rb_2TiEr(PO_4)_3$ appears. This new phase has a langbeinite-type structure like the phases resolved by Masse et al.[19] and Leclaire et al.[20]

When 2 mol % TiO_2 in the solution is substituted by Er_2O_3, the critical concentration of Nb_2O_5 increases as the P_2O_5 concentration increases and the concentration of TiO_2 in the solution decreases. When the critical concentration of Nb_2O_5 is exceeded, the $RbTiPO_5$:Er,-Nb phase appears.

Table 1 also shows the distribution coefficient of the dopants in the crystal. The presence of niobium as a codoping element remarkably enhances the distribution coefficient of Er^{3+}. Moreover, the distribution coefficient of Er^{3+} increases as the P_2O_5 concentration decreases and the concentration of TiO_2 in the solution increases. The distribution coefficient of Nb^{5+} is similar in RTP:Nb and RTP−Er,Nb crystals but increases slightly like the distribution coefficient of Er^{3+} in RTP:Er,Nb crystals. For RTP−Nb crystals, the critical concentration is higher than 14 mol % Nb_2O_5 substituting TiO_2 in the solution selected. The rate of crystal growth decreases and the concentration of crystal defects increases when the concentration of Nb_2O_5 rises.

The presence of Nb in the RTP:Nb and RTP:Er,Nb crystals produces an important change in the morphology of the crystals. They grow as thin plates, where the dimension in the *a* direction is smaller than the crystal dimensions in the *b* and *c* directions. The {100} face is more developed than the other faces of the crystal. These observations agree with previous results.[21] Figure 6 shows the morphology of an RTP and an RTP:Er,Nb crystal drawn with the software Shape.[22]

Figure 7 shows how the concentration of niobium affects the cell parameters and cell volume of the RTP−Nb. The *a* and *b* parameters decrease while *c* increases as the concentration of Nb increases. These lattice-cell changes are different from those for KTP,[6] where the parameter *a* practically does not change for the doping level studied in this work and the parameters *b* and *c* increase as Nb^{5+} doping increases.

(17) Duhlev, R. *Acta Crystallogr. C* **1994**, *C-50*, 1523.
(18) Harrison, W. T. A.; Gier, T. E.; Calabrese, J. D.; Stucky, G. D. *J. Solid State Chem.* **1994**, *111*, 257.
(19) Masse, R.; Durif, A.; Guitel, J. C.; Tordjman, I. *Bull. Soc. Fr. Miner. Cristallogr.* **1972**, *95*, 47.
(20) Leclaire, A.; Benmoussa, A.; Borel, M. M.; Grandin, A.; Raveau, B. *J. Solid State Chem.* **1989**, *78*, 227.
(21) Wang, J.; Liu, Y.; Wei, J.; Jiang, M.; Shao, Z.; Liu, W.; Jiang, S. *Cryst. Res. Technol.* **1997**, *32*, 319.
(22) Dowty, E. *Shape for Windows*, Version 5.0.1, 1995.

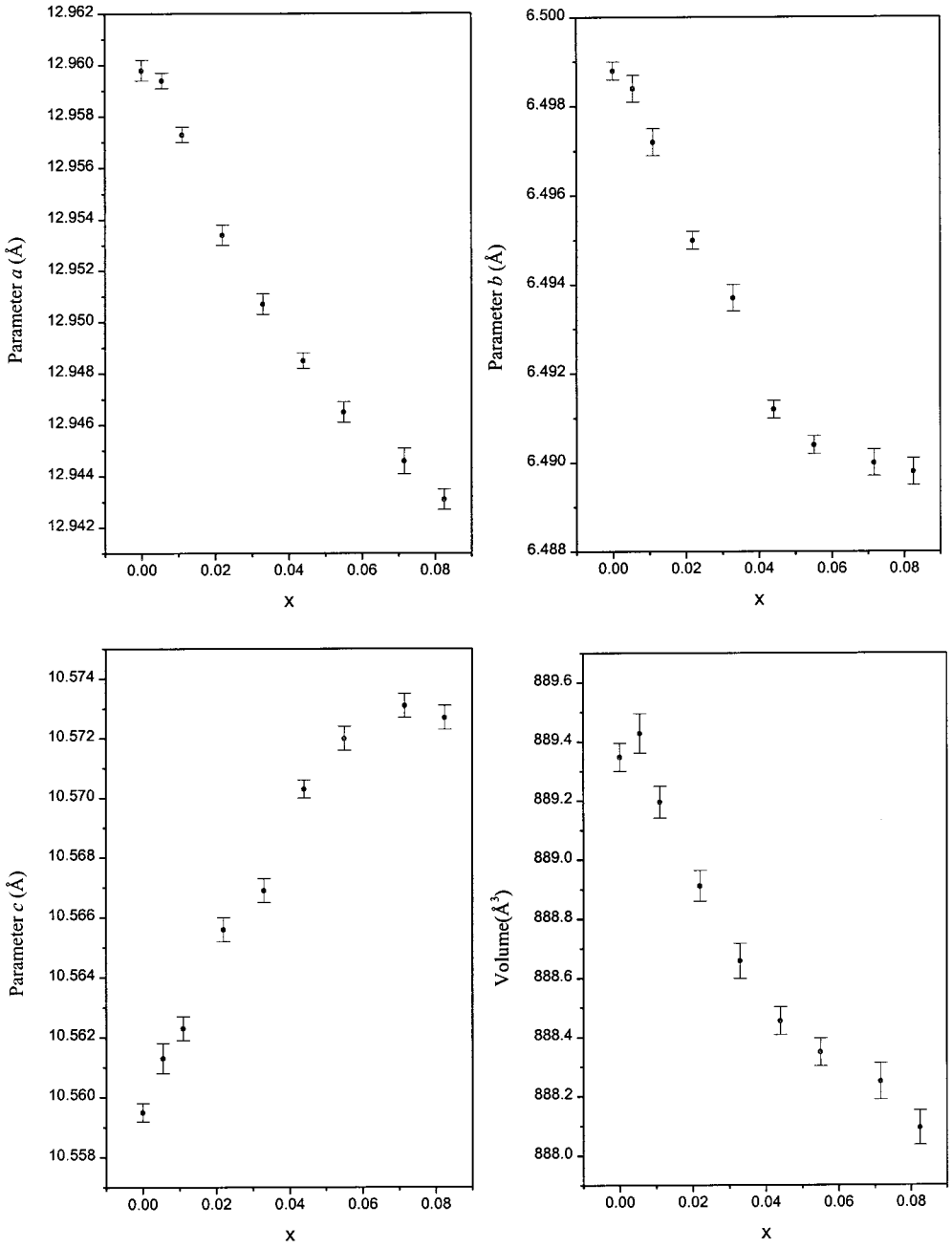

Figure 7. Evolution of the cell parameters and cell volume of the $RbTi_{1-x}Nb_xOPO_4$ crystals as a function of the concentration of niobium.

TSSG of Doped and Codoped RTP Single Crystals. Significant differences in the growth conditions of doped and codoped RTP single crystals in self-fluxes and in fluxes containing WO_3 were observed. In solutions containing WO_3, the time of homogenization is shorter than that in self-fluxes, the cooling of the solution can be made faster, and inclusion-free single crystals can be grown with a seed located in the center of the solution surface without the stirring turbine being needed. As studied in the literature,[23] the viscosity of solutions containing WO_3 is expected to be lower than that in self-fluxes.

In solutions containing Nb_2O_5, the average time of homogenization increases and the average rate of growth of inclusion-free single crystals decreases as the concentration of niobium in the solution increases irrespective of the flux used. In crystals containing Nb, some cracks normally appear in the crystal coming from the seed of RTP. This problem can largely be solved by using seeds of RTP:Nb, as was described in the literature for KTP doped with Nb.[21] In these crystals, the differences between the dimension in the *a* direction and the dimensions in the *b* and *c* directions are significant because the *a* dimension is smaller than the others (see Figure 6). Incorporating Er^{3+}, at least at this low level, scarcely influences the habit in relation to undoped RTP, whereas incorporating Nb^{5+}, even at low levels, influences the habit a great deal, as is explained before.

The results of the experiments to grow RTP:Er, RTP:Nb, and RTP:Er,Nb single crystals are listed in Table

(23) Iliev, K.; Peshev, P.; Nikolov, V.; Koseva, I. *J. Cryst. Growth* **1990**, *100*, 225.

Table 3. Distribution Coefficients of Er, Nb, and W in RTP Crystals

exp no.	K_{Nb}	K_{Er}	K_W
1			
2		0.02	
3	0.56		
4	0.49		
5	0.57	0.04	
6	0.37	0.14	
7	0.62	0.04	
8	0.26	0.06	
9			0.006
10	0.63	0.24	0.01

2. The difference of the saturation temperature (ΔT_s) of the solution before (T_s) and after (T'_s) growth of the crystal was measured. Using these data, the efficiency, defined as

$$\text{efficiency} = \left[\frac{T_s - T'_s}{T_s - T_{final}}\right] \times 100 \qquad (1)$$

where T_{final} is the final temperature of the growth process, was calculated. This efficiency is similar for RTP and RTP:Er when the composition of the basic solution and the growth conditions are the same. When Nb_2O_5 is present in the solution, efficiency decreases quickly as the concentration of Nb_2O_5 increases. For RTP:Er,Nb, four different solution compositions (see experiments 5−8 in Table 2) were studied, and the same growth conditions were maintained (temperature gradient, turbine stirring, cooling rate, etc.) From these experiments, we can see that experiments 5 and 7, which have a higher Rb_2O/P_2O_5 ratio than experiments 6 and 8, are more efficient.

Average supersaturation was obtained from the weight of the crystals, the weight of the initial solution, and $\Delta T_s = T_s - T'_s$. This average is similar for RTP and RTP:Er, but it decreases when the crystals contain Nb^{5+}. As with the efficiency, this average supersaturation decreases as the concentration of Nb_2O_5 in the solution increases. In RTP:Er,Nb crystals whose concentration of Er_2O_3 and Nb_2O_5 that substitutes TiO_2 in the solution is the same, this parameter is similar for all experiments, irrespective of the solution composition (see experiments 5−8 in Table 2). Finally, in experiments in WO_3 fluxes, a similar behavior is observed.

The distribution coefficients of Er and Nb, defined as

$$K_{DE} = \frac{([DE]/([Ti] + [Nb] + [Er]))_{crystal}}{([DE]/([Ti] + [Nb] + [Er]))_{solution}} \qquad (2)$$

where DE is Er or Nb, depending on the experiment, are listed in Table 3. The distribution coefficient of Nb decreases when the concentration of Nb_2O_5 in the solution increases, as can be seen in experiments 3 and 4. In RTP:Er,Nb experiments, this distribution coefficient is higher for crystals grown in solutions containing a higher Rb_2O/P_2O_5 ratio (see experiments 5−8). The distribution coefficient of Er is higher when the solution contains Rb_2O, but unlike the distribution coefficient of Nb, for crystals grown in solutions containing a higher Rb_2O/P_2O_5 concentration ratio, the distribution coefficient of Er is lower. The same coefficients, calculated in crystals grown in fluxes with WO_3, are higher than the coefficients in crystals grown in self-fluxes.

The distribution coefficient of W was calculated from the expression

$$K_W = \frac{([W]/([Ti] + [Nb] + [Er] + [W]))_{crystal}}{([W]/([Ti] + [Nb] + [Er] + [W]))_{solution}} \qquad (3)$$

This increases when Nb_2O_5 is present in the solution.

For solution compositions in the region where the saturation temperature is high, the solution climbs high up the crucible walls and the growth device and evaporation is high. These compositions are therefore not suitable for growing RTP:Er,Nb single crystals.

Optical Absorption. The as grown RTP:Er,Nb samples show a broad band similar to that observed in reduced KTP samples.[24] This absorption overlaps and hides the Er^{3+} bands. To minimize this broad absorption, the RTP:Er,Nb samples were heated for 3 h to 500 °C before the optical measurements. The residual background absorption was subtracted from the spectra.

Figure 8 shows the room-temperature unpolarized optical absorption spectra of Er^{3+} in the RTP:Er,Nb sample. The energy levels of Er^{3+} are characterized by $^{2S+1}L_J$ multiplets whose degeneracy is partially lifted by the host crystal field. This gives rise to Stark sublevels, and the average positions of the multiplets are not very sensitive to the host.[25,26] The optical absorption corresponds to electron transitions from the ground $^4I_{15/2}$ multiplet to the upper energy ones. In the RTP:Er,Nb sample eleven multiplets, namely $^4G_{9/2}$, $^4G_{11/2}$, $^2H_{9/2}$, $^4F_{3/2}$, $^4F_{5/2}$, $^4F_{7/2}$, $^2H_{11/2}$, $^4S_{3/2}$, $^4F_{9/2}$, $^4I_{11/2}$, and $^4I_{13/2}$, can be clearly resolved.

These results show that the RTP:Er,Nb sample spectrum is better defined than RTP:Er sample spectra[27] and shows a higher intensity.

The experimental oscillator strengths, f_{exp}, of the J → J′ transition (J being the $^4I_{15/2}$ fundamental multiplet) are obtained from the experimental spectra by

$$f_{exp} = \frac{2mc}{\alpha_f h N \bar{\lambda}^2} \int_{JJ'} \alpha(\lambda)\, d\lambda \qquad (4)$$

where m is the electron mass, c the vacuum speed of light, α_f the fine-structure constant, h the Planck constant, N the erbium concentration, $\bar{\lambda}$ the average wavelength, and $\int_{JJ'} \alpha(\lambda)\, d\lambda$ the integrated absorption of the J → J′ transition. Table 4 summarizes the integrated optical absorption, the average wavelength considered for each multiplet, and the experimental oscillator strengths obtained using the refractive indices of RTP given by Cheng et al.[28] and $N = 0.65 \times 10^{20}$ atom·cm^{-3}.

For electric dipole transitions, the Judd−Ofelt theory gives the magnitude of the oscillator strengths as a function of the Ω_k (k = 2, 4, 6) Judd−Ofelt parameters.[29,30] The theoretical oscillator strength of electric

(24) Martín, M. J.; Bravo, D.; Solé, R.; Díaz, F.; López, F. J.; Zaldo, C. *J. Appl. Phys.* **1994**, *76*, 7510.
(25) Weber, M. J. *Phys. Rev. B* **1967**, *157*, 262.
(26) Carnall, W. T.; Fields, P. R.; Rajnak, K. *J. Chem. Phys.* **1968**, *49*, 4424.
(27) Rico, M.; Zaldo, C.; Massons, J.; Diaz, F. *J. Phys. Condensed Matter* **1998**, *10*, 10101.
(28) Cheng, L. K.; Cheng, L. T.; Galperin, J.; Morris, P. A.; Bierlein, J. D. *J. Cryst. Growth* **1994**, *137*, 107.
(29) Judd, B. R. *Phys. Rev.* **1962**, *127*, 750.
(30) Ofelt, G. S. *J. Chem. Phys.* **1962**, *37*, 511.

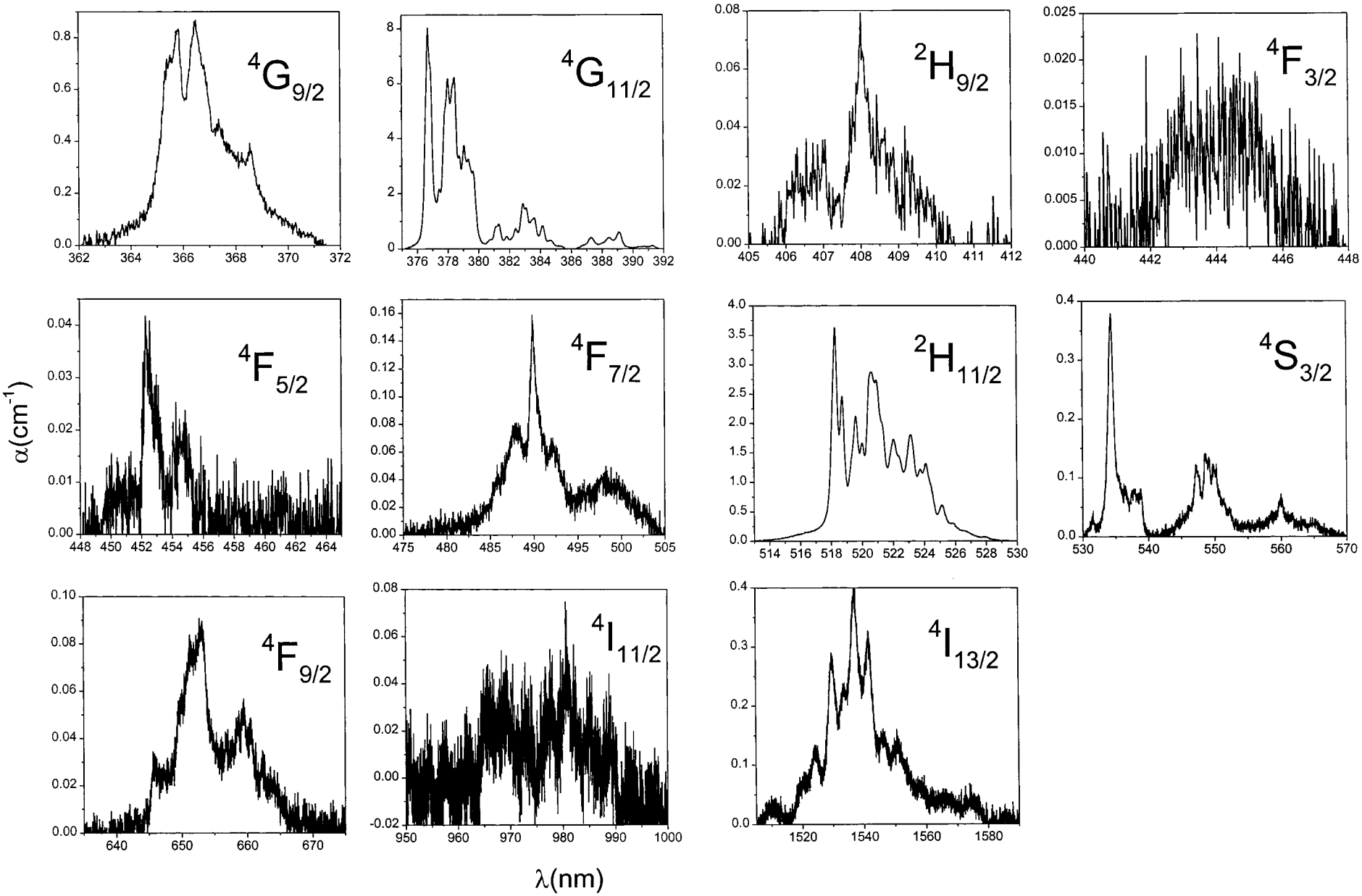

Figure 8. Unpolarized optical absorption spectra of $RbTi_{0.95}Nb_{0.03}Er_{0.02}OPO_4$ crystals at room temperature.

Table 4. Oscillator Strengths, *f*, and Average Wavelength, $\bar{\lambda}$, for Different Multiplets of Er^{3+} in the RTP:Nb,Er Crystal[a]

$^{2S+1}L_J$	$\int\alpha(\lambda)\,d\lambda$	$\bar{\lambda}$ (nm)	$10^7 f_{exp}$	$10^7 f_{theo}$
$4G_{9/2}$	2.41	365.0	31.4	6.27
$^4G_{11/2}$	18.21	380.0	219	196
$^2H_{9/2}$	0.09	408.0	0.95	2.86
$^4F_{3/2}$	0.04	444.4	0.35	1.29
$^4F_{5/2}$	0.09	454.8	0.78	2.21
$^4F_{7/2}$	0.88	494.1	6.28	7.57
$^2H_{11/2}$	13.02	522.0	83.1	103.4
$^4S_{3/2}$	1.74	541.0	10.3	1.80
$^4F_{9/2}$	0.83	649.5	3.39	8.29
$^4I_{9/2}$		805.0		1.39
$^4I_{11/2}$	0.27	974.1	0.50	3.71
$^4I_{13/2}$	7.41	1537.5	5.45	4.80

[a] Note: All the transitions start from the $^4I_{15/2}$ ground state.

Table 5. Second-Harmonic Generation (SHG) Efficiency of $RbTi_{1-x}Nb_xOPO_4$ in Relation with KTP

x	$(\text{SHG efficiency})_{RTP}/(\text{SHG efficiency})_{KTP}$
0	0.73
0.02	0.97
0.04	1.23
0.07	0.73

dipolar transitions, $f_{ED,th}$, is defined as

$$f_{ED,th} = \chi\left[\frac{8\pi^2 mc}{h}\right]\frac{1}{3\bar{\lambda}(2J+1)}\sum_{k=2,4,6}\Omega_k|\langle||U^{\lambda}||\rangle_{JJ'}|^2 \quad (5)$$

where $\chi = (n^2+2)^2/9n$, n is the refractive index, and $\langle||U^{\lambda}||\rangle_{JJ'}$ are the reduced matrix elements corresponding to the JJ' transition of Er^{3+} tabulated by Weber.[25]

The Judd−Ofelt parameters for Er^{3+} in RTP:Nb were obtained by minimizing the difference between the experimental and the calculated oscillator. The quality of the fit is characterized by root-mean-square (rms) deviation. The Judd−Ofelt parameters obtained are $\Omega_2 = 5.99 \times 10^{-20}$, $\Omega_4 = 0.54 \times 10^{-20}$, and $\Omega_6 = 0.37 \times 10^{-20}$ cm^2 with an rms deviation of 1.30×10^{-6}. The values for the Ω_k set are in the range for Er^{3+} in other lattices.[31]

Second-Harmonic Generation. The SHG efficiency is defined as the relation between the powers of the pumping beam (1064 nm) and the green one (532 nm). Table 5 shows the results obtained in the study of the $RbTi_{1-x}Nb_xOPO_4$ ($x = 0$, 0.02, 0.04, and 0.07) crystals. These results are referred to KTP, now that the parameters of KTP are well established in the literature.[16] The SHG efficiency of undoped RTP is slightly lower than that of KTP, as expected from previous reports.[32] Partially substituting Ti with Nb increases the SHG efficiency of RTP up to the values of KTP. This efficiency reaches a maximum for Nb substitution of around 4 atom %. For greater concentrations of Nb, the SHG efficiency decreases and, when the concentration is around 7 atom % of Nb substituting Ti in the crystals, this parameter is similar to that with undoped RTP. We are currently investigating the effect of Nb as a codoping element in RTP to increase the distribution coefficients of different rare earths in the lattice of RTP. Our results seem to indicate that around 3−4 atom % of Nb substituting Ti in the crystals is sufficient in order to allow a reasonable efficiency in the doping process and provides the maximal SHG efficiency. $RbTi_{0.97}Nb_{0.03}OPO_4$, therefore, seems a good choice to host erbium with the aim of obtaining self-induced effects.

Conclusions

The crystallization regions of RTP in the self-flux and in fluxes containing 10, 20, and 30 mol % WO_3 are obtained. A displacement of these crystallization regions to Rb_2O rich ones is observed when WO_3 in the solution increases. This crystallization region is significally narrow with 30 mol % WO_3.

In the Er-doping RTP experiments the critical concentration of Er_2O_3 substituting TiO_2 in the solution was enhanced when the P_2O_5 contents decreased and the TiO_2 contents in the solution increased. In the experiments of RTP doped with Er and Nb, in which the concentration of Er_2O_5 was fixed at 2 mol % substituting TiO_2 in the solution, the critical concentration of Nb_2O_5 decreased as the P_2O_5 concentration decreased and the TiO_2 concentration increased. At the same time, the distribution coefficients of Nb^{5+} and Er^{3+} increased.

The presence of niobium as a codoping element induces an important enhancement of the distribution coefficient of Er^{3+}, both in self-fluxes and in WO_3 fluxes. This is reflected in the high intensity of the room-temperature optical absorption of the $RbTi_{0.95}Nb_{0.03}Er_{0.02}OPO_4$ crystal, which allows the observation of 11 multiplets from a possible total of 12 in the 350−1750 nm spectral region.

The morphologies of the crystals containing niobium and those without it were significantly different. Crystals containing Nb grow with the {100} face more developed than the other faces of the crystal. The presence of Nb_2O_5 in the solution reduces the crystal growth rate and causes crystal defects.

A platinum turbine was used to stir the solution in order to obtain RTP, RTP:Er, and RTP:Er,Nb single crystals in self-fluxes by the TSSG method. When Nb_2O_5 was present in the solution, efficiency and average supersaturation dropped. These parameters are similar when Er_2O_3 is the only dopant used, but they increased in crystals grown in fluxes containing WO_3.

A maximum efficiency of SHG in RTP:Nb is found with about 4 atom % Nb^{5+} substitution of Ti^{4+} in the crystal, followed by a decrease for higher contents of Nb.

Acknowledgment. This work has been supported by CICyT under projects MAT99-1077-C0 and 2FD97-0912-C02 and Generalitat de Catalunya under project 1999SGR 00183. J.J.C. would also like to acknowledge a fellowship from the Generalitat de Catalunya (2000FI 00633 URV APTIND).

CM000305C

(31) Gorller-Walrand, C.; Binnemans, K. *Handbook on the Physics and Chemistry of Rare Earths*; North-Holland Elsevier: 1998; Vol. 25, Chapter 167.

(32) Voronkova, V. I.; Yanovskii, V. K. *Izv. Akad. Nauk SSSR Org. Mater.* **1988**, *24*, 273.